OPTIMAL SHAPE DESIGN OF STRESS RELEASING HOLES

Pauli Pedersen

Department of Mechanical Engineering, Solid Mechanics
Technical University of Denmark
Nils Koppels Allé, Building 404, DK−2800 Kgs. Lyngby, Denmark

Introduction and an illustrating example

The method of hole drilling near the crack tip is often used in fatigue damage repair. In the survey by Shin *et al.* (1996) comparisons with alternative methods are presented and it is concluded that hole drilling was most effective. A number of experimental results are presented. In a recent paper by Thomas *et al.* (2000) optimum location of the drilled holes are discussed. The specific problem of a centre cracked plate is studied with four relatively large holes (20−40 mm) placed symmetrically relative to the crack. Only circular holes are applied.

From shape optimization we know that the circular shape is by no means optimal, see e.g. Pedersen (2000, 2001). It is therefore important to find the shape of a hole, which in the most effective way, releases the stress concentration. A simple parametrization, used in earlier shape optimizations, is applied and it is shown that an almost uniform stress state can be obtained along the boundary of the hole. The shape of the hole is described by the superelliptic equation

$$(x/a)^\eta + (y/b)^\eta = 1 \tag{1}$$

where the x direction is the direction of the crack. If we use a square design domain $a = b$ (supercircle), then the only design parameter is η. We show in figure 1 three designs corresponding to $\eta = 2$ (circular), $\eta = 2.5$ (optimized) and $\eta = 6$. In the figure it is, by the red areas added to the boundary of the hole, illustrated how the strain energy density varies along the boundary of the hole (the same technique is applied in figures 3, 4 and 5). Values for relative maximum strain energy densities for the three designs are 1.00, 0.67 and 1.13 corresponding to relative maximum tangential stresses 1.00, 0.82 and 1.06. We note that considerably better distributions of stresses can be obtained. Even more uniform fields along the hole boundary can be obtained when more design parameters are included.

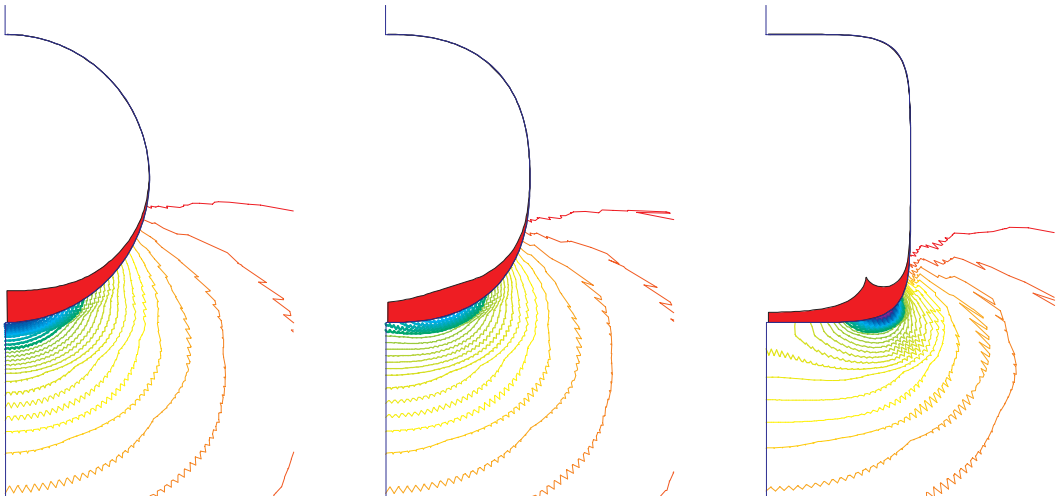

Figure 1: The energy distribution around half the holes, corresponding to $\eta = 2.0$, 2.5 and 6.0.

The objective of the optimal shape design in relation to cracks is not completely clear. At first we may argue that the objective should be to minimize the stress intensity factor. However, for non−sharp crack

tips the interpretation of the stress intensity factor is not clear. Thus we choose to minimize the maximum tangential stress at the boundary of the drilled hole. In the case of plane stress this also corresponds to minimizing the maximum von Mises stress or the energy density. For the cases of non−isotropic materials it seems most relevant to minimize the maximum energy density.

Stresses, stress intensity and energy release

We analyze the elementary case of Isida (1971), shown in figure 2 (the small hatched part corresponds to figure 1). With stress load $\bar{\sigma}$ in the $y-$direction the crack tip field expressed in principal stresses σ_1, σ_2 with direction ψ for the σ_1-direction is

$$\sigma_1 = \sigma\left(\cos\frac{\theta}{2} + \frac{1}{2}\sin\theta\right) \ , \ \sigma_2 = \sigma\left(\cos\frac{\theta}{2} - \frac{1}{2}\sin\theta\right) \ , \ \psi = \frac{\pi}{4} + \frac{3\theta}{4}$$

$$\sigma = K_I/\left(\sqrt{2\pi}\ \sqrt{r}\right) \ ; \ K_I = \bar{\sigma}\sqrt{\pi a}\ f_1\left(\frac{a}{w}\ , \frac{h}{w}\right) \qquad (2)$$

with the geometry factor f_1 available in tables or graphs (for $a/w = 0.4$, $h/w = 0.5$ we find $f_1 = 1.63$). A finite element model (FEM) with a minimum element size of $6 \cdot 10^{-5} w$ and with 17300 degrees of freedom confirms this result. Two alternative methods (not described in the literature) for determining K_I confirm the value of f_1 with great accuracy. In the first method the fracture mechanics model and the FEM are only coupled through the matching of energy in a crack tip domain. In contrast to methods based on the $J-$integral we perform a domain integration (summation) that can be taken directly from a finite element model. In the second method the energy release $G = -d\Pi/da = K_I^2/E$ is found directly from a changed model, say with $\Delta a = a \cdot 10^{-2}$. ($\Pi$ is the total potential).

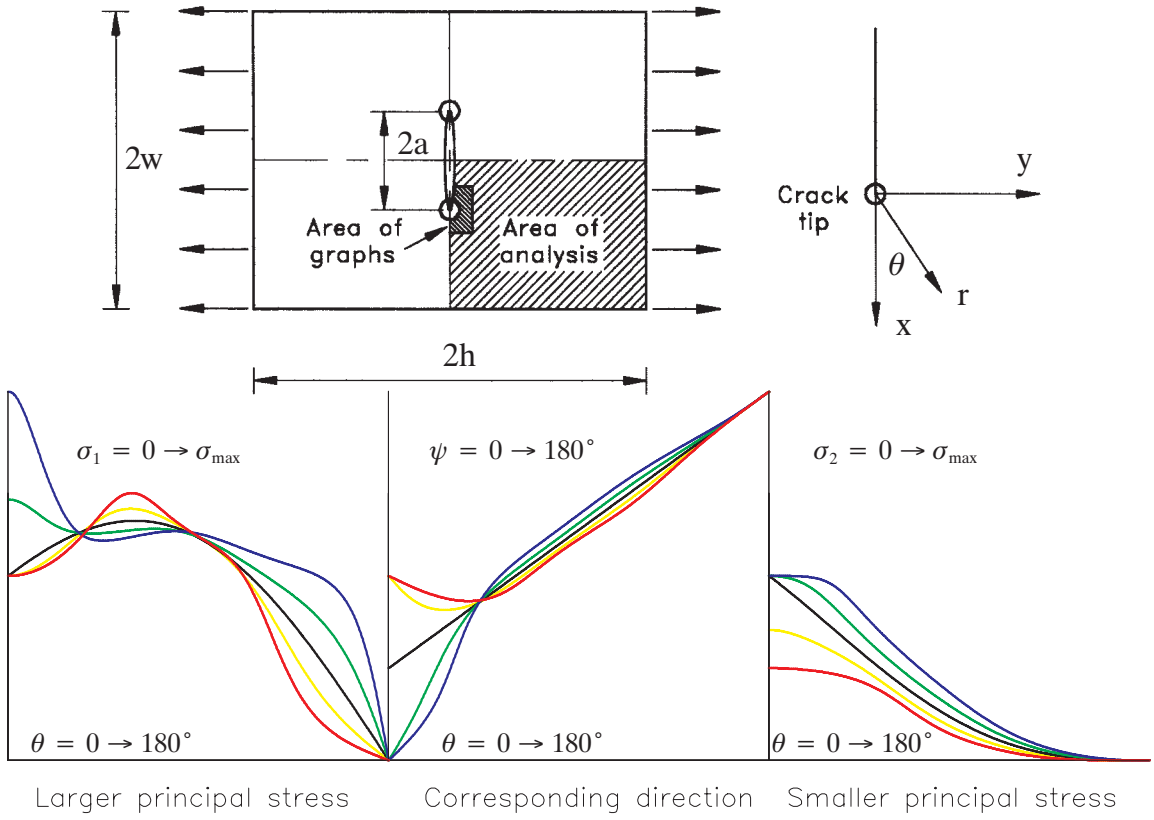

Figure 2: The analyzed elementary case with $w = 100$ mm, indicating also the area of the graphs (hole size $\approx$1 mm). Analytical stress fields at the crack tip (without hole) as a function of θ are shown for four cases of orthotropy and for isotropic material. The colour code is best shown in the σ_2 graph, where from below we have $E_C/E_T = 0.25, 0.5, 1.0, 1.5, 2.0$, respectively.

Because we shall also optimize shapes of holes in orthotropic materials, it may be informative to show a graph of the principal stresses (2) for the extended cases of $E_C/E_T = 0.25\ ,\ 0.50\ ,\ 1.0$ (isotropic) , 2.0 and 4.0 where E_C is the modulus in the crack direction, and E_T is the modulus in the transverse direction. (In all cases we kept the major Poisson ratio $\nu_{CT} = 0.3$ and $E_T/G_{CT} = 2.6$) . By the method described above, the relative K_I values for these cases are determined to $1.35\ ,\ 1.13\ ,\ 1.0\ ,\ 0.90\ ,\ 0.82$, i.e. increasing with increasing flexibility in the crack direction. In figure 2 the actual model is shown together with the fracture mechanics analytical solutions. The blue curve is the isotropic case of eq. (2) and the red curve corresponds to $E_C/E_T = 0.25$, i.e. the case for which optimal shape will be shown.

Sensitivity of the optimal shape

The example shown in the introduction is based on a number of assumptions and a study of the sensitivity to these assumptions is needed.

Influence from the external load and size of the hole. Different external loads can be examined, either given stresses (forces) or given forced displacements. As expected only little influence is seen as long as the crack is loaded mostly in mode I. This follows from the fact that the near crack tip field will, as a function of the external load, only change with a common factor (the stress intensity factor). Optimization for cracks in mode II, mode III and combined modes needs further studies.

In table 1 we show the relative concentration of the energy density, for different size of the holes and for two alternative load cases. In all cases the best of the analyzed designs correspond to a superelliptic power of $\eta = 2.5$. Relative to the size of the hole $(0.5\ ,1.0\ ,1.5$ and 2.0 mm) , with the 1 mm size as reference, we got $1.92\ ,\ 1.00\ ,\ 0.68\ ,\ 0.52$, and larger holes naturally gives a more efficient stress release. The size of the hole is assumed to be determined by alternative considerations.

Shape parameter		$\eta = 2.0$	$\eta = 2.25$	$\eta = 2.5$	$\eta = 3.0$	$\eta = 3.5$	$\eta = 4.0$	$\eta = 4.5$
size	stress load	1.0	0.857	**0.840**	0.876	0.934	0.994	1.05
0.5 mm	displ. load	1.0	0.854	**0.835**	0.863	0.916	0.973	1.03
size	stress load	1.0	0.857	**0.843**	0.894	0.970	1.05	1.13
1.0 mm	displ. load	1.0	0.852	**0.833**	0.875	0.944	1.02	1.09
size	stress load	1.0	0.856	**0.842**	0.895	0.974	1.06	1.14
1.5 mm	displ. load	1.0	0.850	**0.830**	0.872	0.943	1.02	1.10
size	stress load	1.0	0.854	**0.841**	0.894	0.973	1.06	1.15
2.0	displ. load	1.0	0.847	**0.826**	0.866	0.937	1.01	1.09

Table 1: Relative values of maximum energy density (for a circle, $\eta = 2$, the value is set to 1.0) . Corresponding values for stress are equal to the square−root of the shown values. Optimized values are shown in bold.

Influence from material power law non−linearity. In figure 3 is shown results based on analysis with material non−linearity. As expected from earlier results (Pedersen 2001) the optimal shape of the hole is rather insensitive to the power p $(p \leq 1)$ of the non−linearity. We still obtain almost uniform energy density (here von Mises stress) along the boundary of the hole. The isolines show equal levels of reduced stiffness, described by the factor $(\epsilon_e/\epsilon_0)^p$, where ϵ_e is effective strain and ϵ_0 is the corresponding value that gives the transition from linearity to non−linearity. The assumptions behind the calculations leading to the results in figure 3 correspond to deformation theory with a power law of $p = 0.1$. Relative values for these

results are for the squared maximum von Mises stress 1.0 , 0.98 , 1.11 and for the minimum stiffness reduction factors 0.305 , 0.336 , 0.280 .

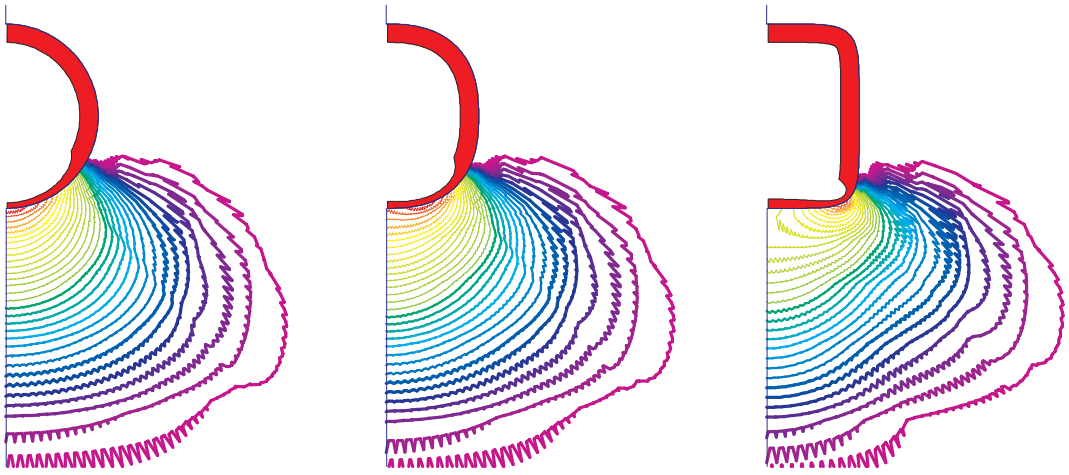

Figure 3: Isolines of stiffness reduction based on material non−linearity. The three designs correspond to $\eta = 2.0$, 2.5 and 6.0 as in figure 1.

Influence from material anisotropy. It is expected that anisotropic material behaviour will influence the optimal shape to a large extend, see Pedersen, Tobiesen and Jensen (1992). When the material is stiffer in the crack direction we see little influence on the optimal shape, but when it gets more flexible in the crack direction the influence is important. We have illustrated this in figure 4, where the ratio of the two moduli is set to $E_C/E_T = 0.25$.

The left most design is the optimized design of $\eta = 2.5$ from the isotropic case, which with only one design parameter (η) is improved to the middle design of $\eta = 4.0$. We note that an energy concentration will always appear for these pure superelliptic designs. With one modification function to the shape of the hole, as described in details in Pedersen *et al*. (1992), we obtain the right most design with almost uniform energy density along the hole boundary. Actual relative maximum values of energy density for the three cases are 1.0 , 0.98 , 0.78 and for maximum principal stresses the values are 1.0 , 0.91 , 0.89 . A study of the stress fields shown in figure 2 (see especially the red σ_1 curve), may give an understanding for the need of more advanced designs for these cases. From the results, the two parameter description seems sufficient.

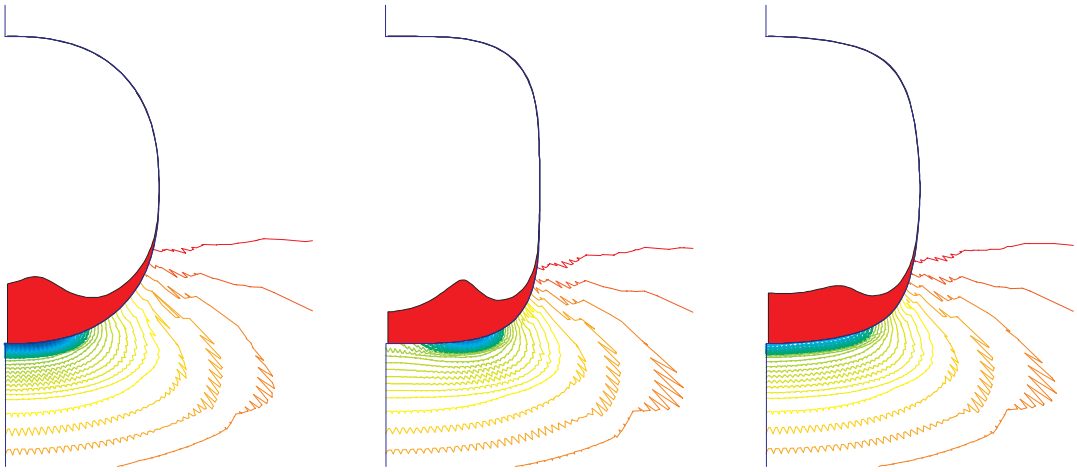

Figure 4: Levels of energy density for $E_C = 0.25E_T$ corresponding to superelliptic design with $\eta = 2.5$ to the left and $\eta = 4.0$ in the middle. The design to the right is a two parameter design with $\eta = 4.0$ and one modification function.

Influence from the domain of the hole. By including the elliptic halfaxes a , b as design parameters (the added condition of $a \cdot b$ = constant practically fixes the area of the hole), we may improve the optimal design results further. In figure 5 are shown the results corresponding to a/b = 1.0 , 0.9 , 0.8 , 0.7 , 0.6 , and 0.5 , illustrating the levels of squared von Mises stress. Note that in all cases we obtain almost uniform distribution along the highly stressed boundary. The resulting relative maximum values are 1.0 , 0.92 , 0.84 , 0.75 , 0.66 and 0.59 , and thus the superellipse has distinct advantages over the supercircle. The optimal superelliptic power η change with the ratio a/b and for the solutions shown, we got η = 2.5 , 2.4 , 2.3 , 2.15 , 2.10 , 1.95 , respectively.

The same six designs were analyzed based on a strong material non−linearity $(\sigma_e/\sigma_0)^{10}$ and again almost constant von Mises stress were obtained along the boundary, although now decreased with almost a factor of four. Relative to the results given for the linear solution, the values with the non−linear solution were 0.24 , 0.23 , 0.22 , 0.21 , 0.20 , 0.18 , respectively. The strong non−linearity levels out the difference, but still the possibility for smaller ratios a/b gives a better solution.

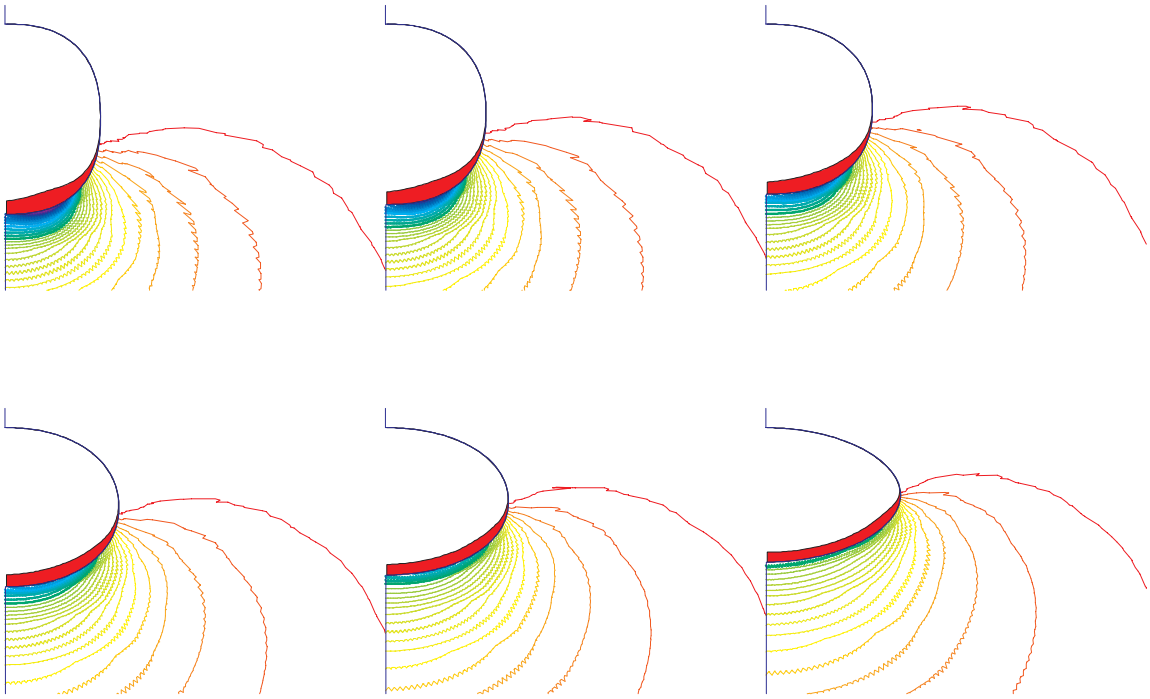

Figure 5: Levels of squared von Mises stress for optimized superelliptic power, when the ratio a/b of elliptic axes are prescribed to 1.0 , 0.9 , 0.8 / 0.7 , 0.6 , 0.5 , respectively.

Conclusion

With illustrative examples we have shown that the stress field, at the boundary of a drilled stress releasing hole, can be significantly improved. To a large extend the one parameter superelliptic shape is able to return a field of constant tangential stress along the boundary. This will diminish the possibility for further fatigue crack initiation.

References

Isida, M., Effect of width and length on stress intensity factors of internally cracked plates under various boundary conditions, *Int. J. of Fracture* **7**, 301–316, 1971.

Pedersen, P., On optimal shapes in materials and structures, *Struct. Multidisc. Optim.* **19**, 169–182, 2000.

Pedersen, P., On the influence of boundary conditions, Poisson's ratio and material non–linearity on the optimal shape, *Int. J. Solids Structures* **38**, 465–477, 2001.

Pedersen, P., Tobiesen, L. and Jensen, S.H., Shapes of orthotropic plates for minimum energy concentration, *Mech. Struct. Mach.* **20**(4), 499–514, 1992.

Shin, C.S., Wang, C.M. and Song, P.S., Fatigue damage repair: a comparison of some possible methods, *Int. J. Fatigue* **18**, 535–546, 1996.

Thomas, S.B., Mhaiskar, M.J. and Sethuraman, R., Stress intensity factors for circular hole and inclusion using finite element alternating method, *Theoretical and Applied Fracture Mechanics* **33**, 73–81, 2000.